RESEARCH

Risk assessment of floor water inrush based on TOPSIS combined weighting model: a case study in a coal mine, China

Qiang Li[1] · Cunjin Lu[1] · Hui Zhao[1]

Abstract

This paper presents a novel water inrush risk index (WIRI) evaluation model based on principal component analysis (PCA), criteria importance though inter-criteria correlation (CRITIC) and technique for order preference by similarity to an ideal solution (TOPSIS). Treating Xinyugou coal mine as the study area, the water inrush risk of coal mining on confined water was evaluated. Seven factors were selected to construct the water inrush evaluation system. The PCA, the CRITIC and the kullback information concept (KIC) were adopted to determine the combination weights of water inrush evaluation indicators. Combined with the TOPSIS method, a WIRI evaluation model was constructed. Also, the geographic information system (GIS) was used to partition the water inrush risk in the study area. The results show that the PCA and the CRITIC were applied in the determination of each evaluation index weight, ensuring the objective presentation of the original information included in the evaluation indicators. Meanwhile, the KIC ensured the scientific construction of combination weight without the occurrence of the weight bias phenomenon; the prediction accuracy of WIRI evaluation model is more than 90%, with a good fitting effect with the actual water inrush points. Compared with the water inrush coefficient method, the model, with five regions classified in the study area, can more intuitively reflect the water inrush risk of each region. This model has a guiding role in preventing water inrush from coal seam floor above confined water.

Introduction

Coal, accounting for 56.8% of energy, is widely used in the daily production and living (Duan and Zhao 2021). China, as one of the largest countries in coal production and consumption, plays an important role in the generation of coal energy. Nearly 60% of the coal resources are produced in the Carboniferous and Permian North China-type coal fields.

✉ Cunjin Lu
tshjlcj@126.com

Qiang Li
qianglicumt@126.com

Hui Zhao
1040453197@qq.com

1 School of Resources and Geosciences, Institute of Mine Water Hazards Prevention and Controlling Technology, China University of Mining and Technology, Xuzhou 221116, China

Especially, these coal seams are often accompanied by the strong water yield limestone aquifers such as the Ordovician limestone aquifers. With the increase of the mining depth, disasters frequently occur under the complex geological conditions (Chen et al. 2018). Among them, the water disaster, ranked second in the coal mine disasters, has always plagued the coal mine safe production (Donnelly 2006; Mahato et al. 2018). In the past few decades, 1184 water accidents occurred in China, with 4735 deaths. These water disasters have caused a large number of casualties and property losses (Wang and Park 2003). Therefore, it is an important task to scientifically predict the coal seam floor water inrush above confined water.

Many scholars have carried out substantial research on the floor water disasters, promoting a series of theories and industry standards. The Slesarev formula, a formula of safe water pressure, regards the floor as a beam with uniform load and both ends fixed. The maximum water pressure value acting on the beam was regarded as the safe water pressure value (Liu et al. 2018a). the floor was divided into three zones in the down three zones theory, namely, the fissure

zone, the intact strata zone and the confined water conductive zone. Among them, the intact strata zone has an inhibitory effect on water inrush (Hu et al. 2021). The rock strata with the strongest bearing capacity between the floor and the aquifer was served as the key strata in key strata theory. Its breaking mechanism has a certain relationship with the law of water inrush (Wang et al. 2021). The floor failure depth theory is the development depth of the floor water conducting fracture zone, deduced from the semi-infinite body theory and the slip field theory (Liu et al. 2018b). The water inrush coefficient, a ratio of the water pressure to the thickness of aquifuge, was treated as the criterion for judging whether the water inrush occurs. It is widely applied in the water inrush evaluation of coal mines (Sun et al. 2020). However, with the deepening of coal mining depth, the complex geological conditions exacerbate the occurrence of water inrush accidents. Only considering these two indicators to measure water inrush is often inconsistent with the actual situation. In addition, the floor water inrush is a geological phenomenon under the combined action of multi information (He et al. 2021). The complexity of the factors, the inconsistency of the dimensions, and the simultaneous development of both qualitative and quantitative factors pose challenges to the decision-making technology of the floor water inrush.

In recent, the multi-criteria decision-making (MCDM) was applied to the water inrush assessment. Hu et al. (2019) constructed a water inrush prediction model to evaluate the water inrush risk of Qiuji coal mine working face, combining AHP and EWM. Niu et al. (2020) adopted the linear weighting method to construct an improved water inrush coefficient model to predict the risk of coal seam floor water inrush on the limestone aquifer. The number, complexity and feature extraction of coal seam floor water inrush factors increase the difficulty of these evaluation methods in the operation process. The PCA reduces the dimensions of many factors affecting the floor water inrush to extract the principal components. It avoids the problems caused by excessive information. Shi et al. (2015) adopted the PCA and the machine learning methods to induce and extract the influencing factors of floor water inrush. Ju and Hu (2021) established a water inrush identification model to study the water inrush risk of Xieqiao coal mine on the basis of PCA method and grey situation decision method. Li et al. (2020) established an identification model of floor water inrush source, combining PCA and Fisher discriminant analysis. It eliminates the overlapping influence between indicators, resulting in an improvement of the identification accuracy of water inrush sources. Zhang et al. (2022) proposed a BP neural network prediction model of water inrush based on PCA and depth confidence network (DBN) to predict the risk of water inrush in actual working face. In addition, the PCA plays a certain role in the analysis of mine water source pollution degree

and the identification of water diversion channel (Salifu et al. 2012; Liu et al. 2019). In MCDM, the method such as AHP was used to divide weights according to expert experience. The preference of experts will lead to uncertainty of weights (Zhang et al. 2021). To eliminate subjective uncertainty, the entropy weight method was applied to determine the weight of water inrush influencing factors in water inrush evaluation (Gao et al. 2022). Compared with subjective evaluation method, the entropy weight method is more accurate and objective. However, the traditional entropy weight method has limitations because of ignoring the conflict between indicators. It is characterized by instability. To eliminate the impact of this deficiency, the CRITIC, considering the conflicts between indicators, was used to determine the weight of indicators (Zhang et al. 2020). Also, this method plays an important role in the identification of water inrush sources (Casagrande et al. 2020). Meanwhile, multiple methods were utilized for constructing combined weights (Wu et al. 2021a). However, the weight coefficients of these methods are often calculated by the linear weighting and the multiplicative weighting. Because of the imbalance of preferences, it may not reflect the comprehensive weight of indicators more accurately. The KIC can constrain the difference of weights determined by various decision methods, improving the accuracy of the combination weight (Osses et al. 2013). Moreover, the comprehensive evaluation includes multiple methods, such as fuzzy comprehensive evaluation (Zhou et al. 2022), composite index method (Yu et al. 2022), attribute mathematics theory (Xu et al. 2021), TOPSIS (Shi et al. 2020), evidence theory (Li et al. 2021), set pair analysis (Li et al. 2018) and matter element analysis (Zhang et al. 2019). In terms of dealing with multiple attribute factors, the TOPSIS can better solve the problem of inconsistent factor dimensions. At the same time, the ideal solutions are delimited to rank the evaluation samples. This method was widely used in the evaluation of water abundance and water inrush (Qiu et al. 2020; Qu et al. 2021). The decision-making of coal seam floor water inrush often involves spatial information related to decision-making information. The decision problem uses multi standard decision analysis in the spatial domain to evaluate the schemes and standards (Yang et al. 2018). GIS, an information processing tool, has the ability to automate, manage and analyze various spatial data (Liu et al. 2020). The decision-making information can be obtained from the geographical data. It can better reflect the spatial information of floor water inrush after being processed by a variety of standards (Wu et al. 2017).

In consideration of the above researches, the current study aims to construct a combined weighted WIRI evaluation model based on the TOPSIS method. The employ of PCA and CRITIC ensures the objectivity of weights, avoiding the loss of indicator information and reflecting the relevance of indicators. The application of KIC improves the scientificity

of the construction of combined weights. The WIRI evaluation model can reflect the water inrush risk degree of the samples. This model can provide guidance for coal mining planning and water disaster prevention.

Study area

Xinyugou coal mine is located in Jiexiu city, Shanxi province, with a mine field area of 9.56 km². The mining elevation ranges from 1060 m asl to 200 m asl. The mine field is situated at the junction of the hilly area on the northern edge of Taiyue mountain and Jinzhong basin. The terrain is generally high in the south and low in the north (Fig. 1). The Zhangjian river runs through the mine field from south to north, with a length of 3.1 km. The highest flood level of it ranges from 1020 m asl to 910 m asl. The well-field has a semi-arid continental monsoon climate in the north warm temperate zone, with an obvious Continental climate features.

Geological conditions

According to the drilling and ground geological data, the strata of the mine field from old to new are the Ordovician, the Carboniferous, the Permian and the Quaternary,

respectively. An anticline is located on the east side of the mine field, with a formation dip ranging from 10° to 20°. The fault structure is developed, without the founding of collapse column and magmatic rock intrusion. The main coal-bearing strata in the mine field are the Lower Permian Shanxi formation and the Upper Carboniferous Taiyuan formation. The No. 9 coal seam, as one of main mineable coal seams, occurs in the Carboniferous Taiyuan formation, with a thickness ranging from 0.3 m to 3.25 m.

Hydrogeological conditions

The main aquifers in the study area are the Ordovician carbonate karst fissure aquifer, the Carboniferous clastic rock, carbonate karst fissure aquifer, the Permian clastic rock fissure aquifer and the Quaternary loose rock pore aquifer (Fig. 2). Among them, the water level buried depth of the Ordovician karst aquifer is 59.50 m. The water level elevation is 911.22 m asl. The Ordovician karst aquifer is characterized by poor-medium water abundance, with a unit inflow ranging from 0.0772 L/s·m to 0.1431L/s·m. The main aquifuge in the study area is the Benxi Formation of the Middle Carboniferous. Its lithology is aluminous mudstone, with a general thickness of 15 m. The Upper Carboniferous and the
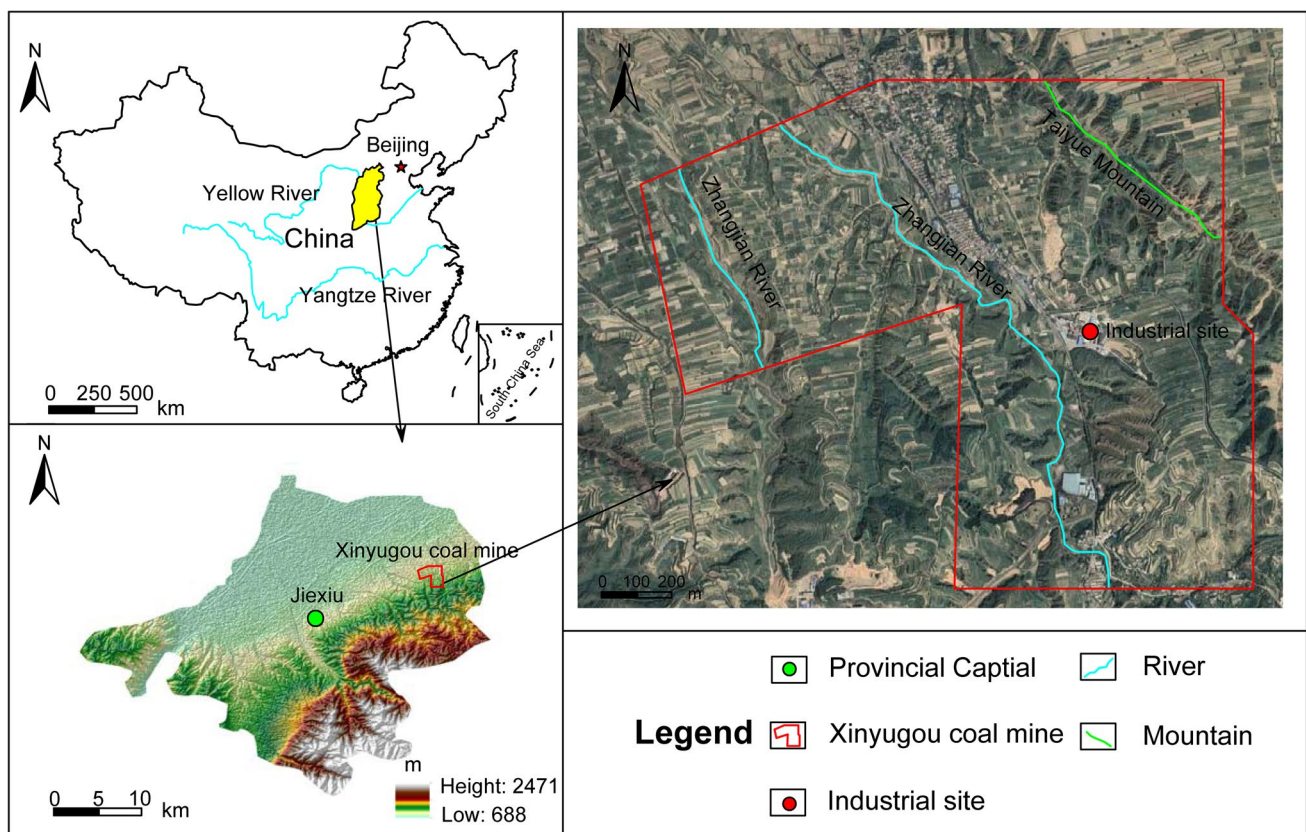

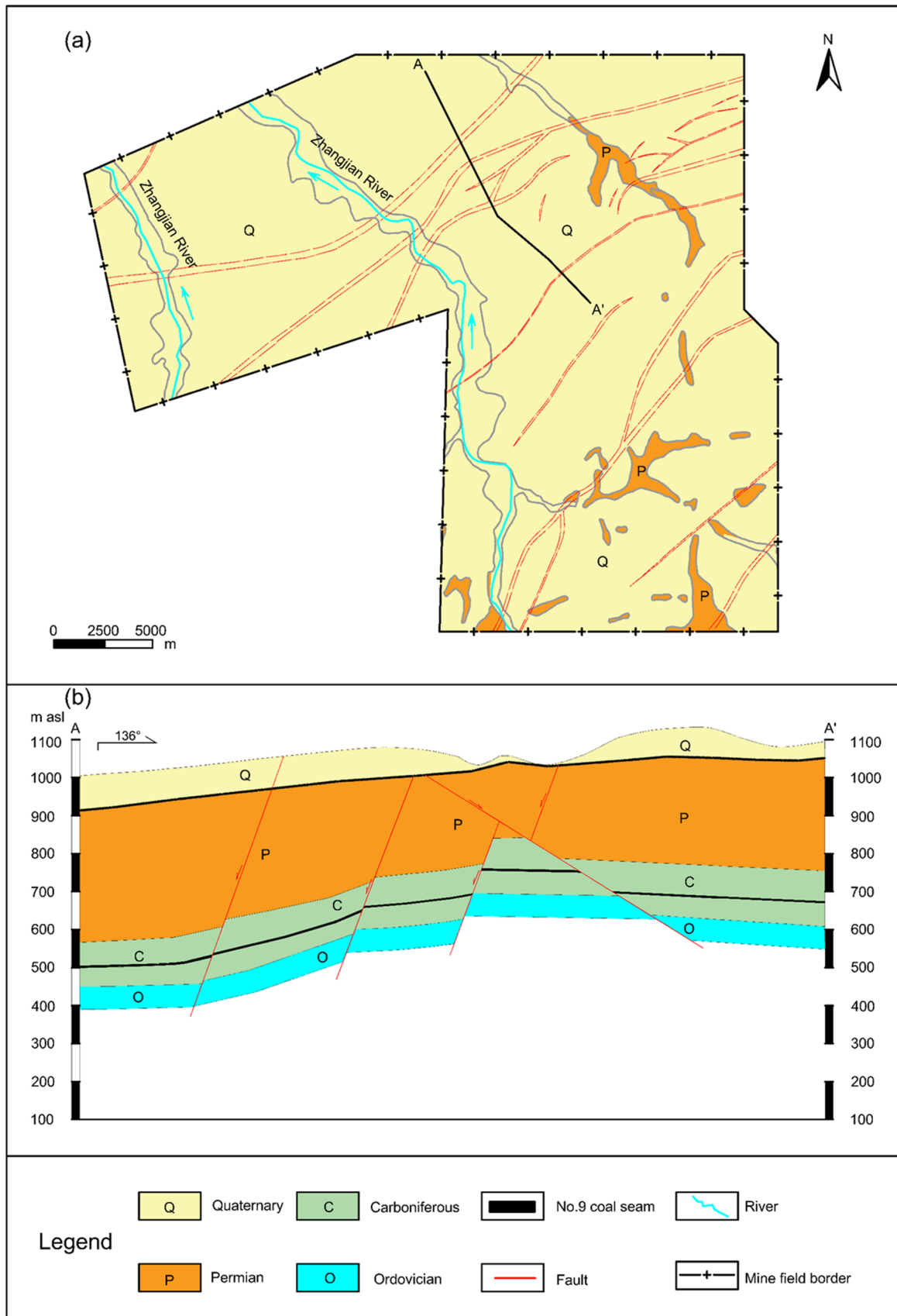**Fig. 1** Location of study area

Fig. 2 Hydrogeological distribution of the study area

Lower Permian are mainly composed of plastic mudstone and sandy mudstone, with a thickness generally ranging from 2.00 to several meters. The No. 9 coal seam, located above the Ordovician aquifer, was threatened by confined water. Therefore, the risk of floor water inrush was taken as the research object of this paper.

Methods

A WIRI evaluation model was constructed based on TOPSIS to evaluate the risk of water inrush on the karst aquifers. It mainly includes the following steps (Fig. 3): (1) Selection of the water inrush evaluation indicators (2) Determination of the weight of the evaluation index (3) Building of the WIRI evaluation model (4) Evaluation and verification of model results.

Selection of water inrush evaluation indicators

The construction of the evaluation index system plays a crucial role in the water inrush evaluation. The evaluation results are affected by the selection of the evaluation index. Thus, we selected 7 factors as the evaluation indicators, considering the geological conditions, the hydrogeological conditions and the mining activities, i.e., the fault fractal dimension, the coal seam dip angle, the mining depth, the slope length of panel, the aquifuge thickness, the water pressure and the water abundance. Also, the single factor thematic maps (Fig. 4) were drawn combined with the geospatial information of each sample data. The effect of evaluation indicators on water inrush was divided into two types: the positive correlation and the negative correlation. Among them, the factors positively related to the risk of water inrush are the fault fractal dimension, the coal seam dip angle, the mining depth, the slope length of panel, the water pressure and the water abundance. While, the factor negatively related to the risk of water inrush is only the aquifuge thickness.

PCA

The PCA, proposed by Pearson (1901), carries out the dimension reduction to transform linearly dependent original
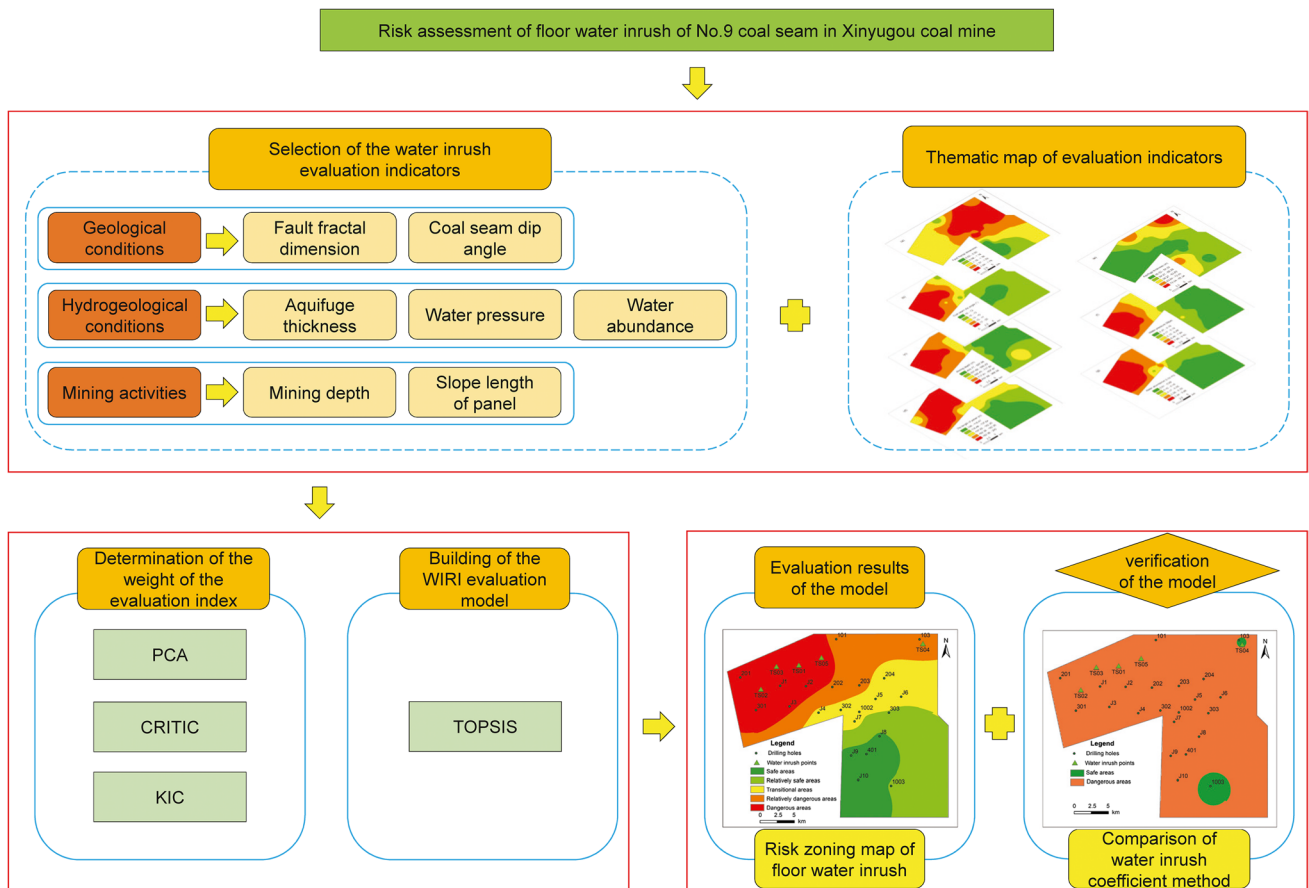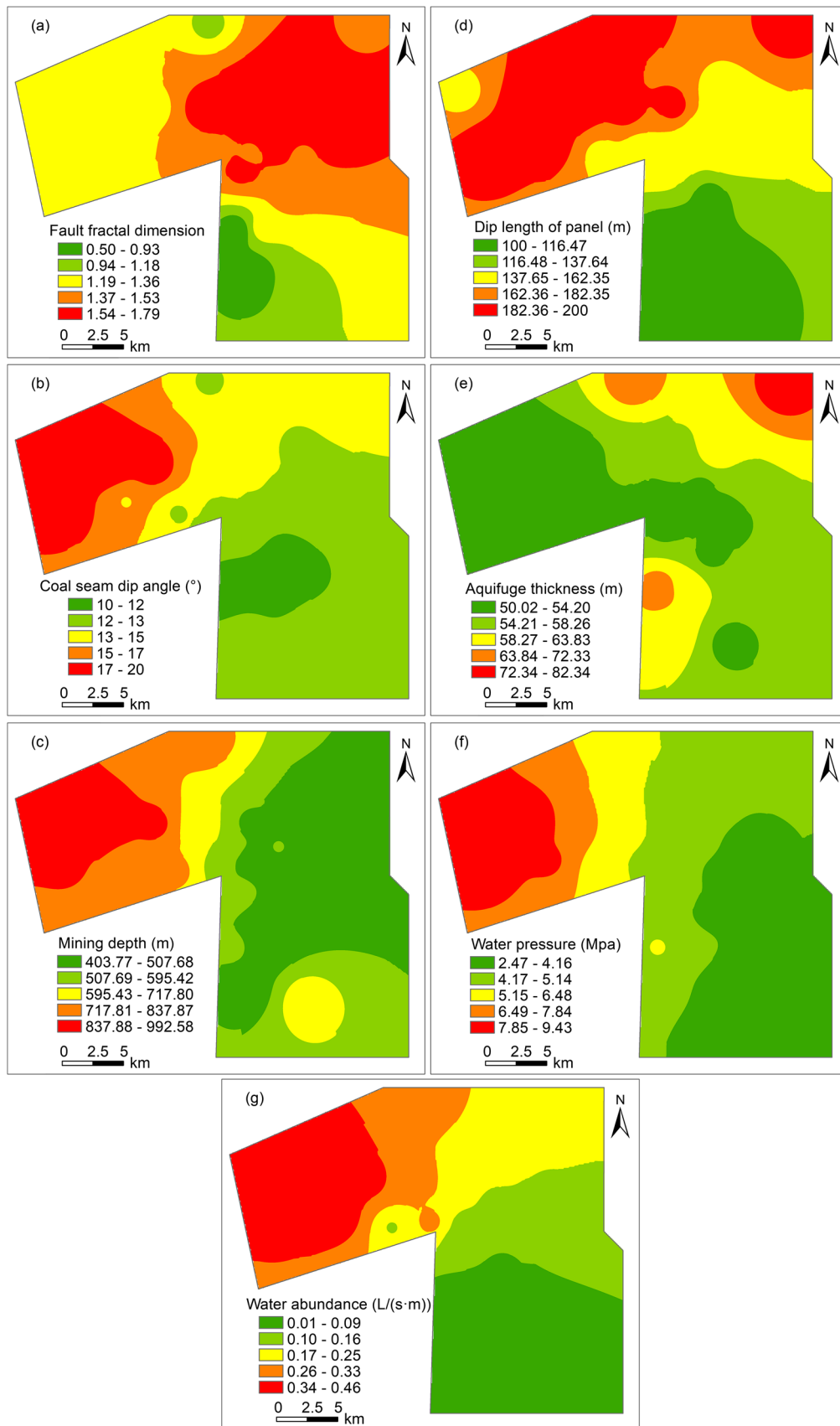

Fig. 3 Flowchart of the research method

Fig. 4 Thematic map of evaluation indicators

variables into independent new variables. The weight determination specific steps of PCA are as follows:

Data standardization. The original data matrix $E = (e_{ij})_{m \times n}$ is constituted by m samples and n evaluation indicators. The standard data matrix $F = (f_{ij})_{m \times n}$ is constructed as follows:

$$f_{ij} = \frac{e_{ij} - \overline{e_j}}{\sigma_j} \tag{1}$$

where e_{ij} is the standard value of i samples on j evaluation indicators; $\overline{e_j}$ is the mean value of jth evaluation indicators, $\overline{e_j} = \sum_{i=1}^{m} e_{ij}/m$, $i = 1, 2, \ldots, m$, $j = 1, 2, \ldots, n$; s_j is the standard deviation of jth evaluation indicators, $\sigma_j = \sqrt{\sum_{i=1}^{m} (e_{ij} - \overline{e_j})^2/m - 1}$, $i = 1, 2, \ldots, m$, $j = 1, 2, \ldots, n$.

Construction of correlation matrix. The correlation matrix G is calculated as follows:

$$G = (g_{ij})_{n \times n} = \begin{pmatrix} g_{11} & g_{12} & \cdots & g_{1n} \\ g_{21} & g_{22} & \cdots & g_{2n} \\ \vdots & \vdots & \ddots & \vdots \\ g_{n1} & g_{n2} & \cdots & g_{nn} \end{pmatrix} \tag{2}$$

where

$g_{ij} = \sum_{k=1}^{n}(f_{ki} - \overline{f_i})(f_{ki} - \overline{f_j})/\sqrt{\sum_{k=1}^{n}(f_{ki} - \overline{f_i})^2}\sqrt{\sum_{k=1}^{n}(f_{kj} - \overline{f_j})^2}$.

Extraction of principal components. The principal component coefficient matrix $H = (h_{ij})_{m \times n}$ is defined through the outcome of the eigenvalues and eigenvectors of the correlation matrix. Further, the corresponding principal component expression is established as follows:

$$\begin{cases} Y_1 = h_{11}X_1 + h_{12}X_2 + \ldots + h_{1n}X_n \\ Y_2 = h_{21}X_1 + h_{22}X_2 + \ldots + h_{2n}X_n \\ \ldots \\ Y_m = h_{m1}X_1 + h_{p2}X_2 + \ldots + h_{mn}X_n \end{cases} \tag{3}$$

where Y_1, Y_2, …, Y_m are principal components; h_{mn} is the principal component score coefficient; and X_1, X_2, …, X_n are standard values.

Weight determination. The calculation of weight mainly includes the following steps: the calculation of each index scores in the principal components are carried on, combined the extracted characteristic values of the principal components with the coefficients in the linear relationship of the principal components; the score coefficients of the principal component in the model are defined (Eq. (4)), combined the each index score in the principal component with the corresponding variance contribution rate of the principal component; the

score coefficient is normalized to obtain the weight value of each index (Eq. (5)).

$$\chi_i = \left| \frac{\sum_{i=1}^{m} \gamma_i \delta_i}{\sum_{i=1}^{m} \delta_i} \right| \tag{4}$$

$$\alpha_i = \frac{\chi_i}{\sum_{i=1}^{m} \chi_i} \tag{5}$$

where χ_i is the score coefficient of the principal component. δ_i is the corresponding variance contribution rate of the principal component, $\delta_i = \lambda_i / \sum_{i=1}^{m} \lambda_i$; γ_i is the score of each index in the principal component, $\gamma_{ij} = h_{ij}/\sqrt{\lambda_i}$, λ_i is the eigenvalue of the correlation matrix, $i = 1 \sim m$, $j = 1 \sim n$. α_i is the weight of the water inrush evaluation index.

CRITIC

The CRITIC is a more scientific objective weighting method (Diakoulaki et al. 1995). It determines the index weight according to the contrast intensity and conflict between the evaluation indicators. Also, the difference and correlation between the indicators is considered. The calculation steps are as follows.

Standardization of evaluation indicators. According to the effect of evaluation index on water inrush, the standardized equations are classified into the positive correlation and the negative correlation.

$$e_{ij}^* = \frac{e_{ij} - \min(e_{ij})}{\max(e_{ij}) - \min(e_{ij})} \tag{6}$$

$$e_{ij}^* = \frac{\max(e_{ij}) - e_{ij}}{\max(e_{ij}) - \min(e_{ij})} \tag{7}$$

where e_{ij}^* is the standardized data; e_{ij} is the original data; $\min(e_{ij})$ and $\max(e_{ij})$ are the minimum and maximum values of each evaluation index, respectively.

Calculation of standard deviation and correlation coefficient. In CRITIC, the standard deviation and correlation coefficient are applied to represent the difference and conflict between indicators, respectively. The larger the standard deviation, the greater the difference between the indicators. A positive correlation coefficient indicates that the conflict between the indicators is smaller. The standard and correlation coefficients between indicators are calculated as follows:

$$S_j = \sqrt{\frac{\sum_{i=1}^{m}(e^*{}_{ij} - \overline{e^*{}_j})^2}{m - 1}} \tag{8}$$

$$r_{kl} = \frac{\sum_{i=1}^{m}(e^*{}_{ik} - \overline{e^*{}_k})(e^*{}_{il} - \overline{e^*{}_l})}{\sqrt{\sum_{i=1}^{m}(e^*{}_{ik} - \overline{e^*{}_k})^2 \sum_{i=1}^{m}(e^*{}_{il} - \overline{e^*{}_l})^2}} \tag{9}$$

where $\overline{e^*{}_j}$ is the mean value of the jth evaluation indicators; r_{kl} is the correlation coefficient between evaluation indicators, $k = 1, 2, …, n$; $l = 1, 2, …, k$.

Determination of indicators conflict. The conflict between evaluation indicators is calculated as follows:

$$R_j = \sum_{k=1}^{n}(1 - r_{kl}) \tag{10}$$

where R_j is the conflict of the jth evaluation index.

Calculation of evaluation index information amount and weight. The information amount and weight of the evaluation index are determined by Eqs. (11) and (12), respectively.

$$t_j = S_j R_j \tag{11}$$

$$\beta_j = \frac{t_j}{\sum_{j=1}^{n} t_j} \tag{12}$$

where t_j is the information amount of jth evaluation index; β_j is the weight of jth evaluation index.

KIC

To make the combination weight as close as possible to the weights of two methods, the objective function of the combination weight is constructed by the KIC (Thiesen et al. 2019). Also, the combination weight of the evaluation index can be obtained by the Lagrange multiplier method.

$$\begin{cases} \min J(w) = \sum_{j=1}^{n} \left(w_j \ln \frac{w_j}{\alpha_j} + w_i \ln \frac{w_j}{\beta_j} \right) \\ \text{s.t.} \sum_{j=1}^{n} w_j = 1, w_j \geq 0, i = 1, 2, \cdots, n \end{cases} \tag{13}$$

$$w_j = \frac{\sqrt{\alpha_j \beta_j}}{\sum_{j=1}^{n} \sqrt{\alpha_j \beta_j}} \tag{14}$$

where w_j is the combination weight of the jth evaluation index.

TOPSIS

The TOPSIS, also known as the distance method of superiority and inferiority, commonly used in the multi-objective decision analysis (Baykasoğlu and Gölcük 2017; Norouzi and Namin 2019). Its basic principle is to sort by detecting the distance between the evaluation object and the optimal solution and the worst solution. If the evaluation object is closest to the optimal solution and furthest away from the worst solution, it is the best; Otherwise, it is not optimal. The specific steps are as follows:

Construction of weighted standardization matrix. The weighted standardization matrix $R^* = (r^*_{ij})_{m \times n} = (w_j e^*_{ij})_{m \times n}$ is constructed on the basis of the combined weight and standardized values of evaluation index.

Definition of positive and negative ideal solutions of water inrush. There is a certain relationship between the evaluation index and water inrush. A larger negative correlation index value implies a lower probability of water inrush; a larger the positive correlation index value indicates a higher probability of water inrush. Thus, the negative ideal solution of water inrush is the minimum value of positive correlation index or the maximum value of negative correlation index. However, the positive ideal solution of water inrush is opposite. The determination equations are as follows:

$$C^- = \left\{ \left(\max r^*_{ij} | j \in \gamma_1 \right), \left(\min r^*_{ij} | j \in \gamma_2 \right) \right\} \tag{15}$$

$$C^+ = \left\{ \left(\min r^*_{ij} | j \in \gamma_1 \right), \left(\max r^*_{ij} | j \in \gamma_2 \right) \right\} \tag{16}$$

where C^- is the negative ideal solution; C^+ is the positive ideal solution; γ_1 is the negative correlation index collection; γ_2 is the positive correlation index collection.

Determination of water inrush index. The distance from the ith sample to the negative ideal solution and the positive ideal solution are calculated as follows:

$$D_i^- = \sqrt{\sum_{j=1}^{n}(r^*_{ij} - c^-_{ij})^2} \tag{17}$$

$$D_i^+ = \sqrt{\sum_{j=1}^{n}(r^*_{ij} - c^+_{ij})^2} \tag{18}$$

Table 1 Corresponding contribution rates of each component

Component	Eigenvalues	Variance contribution rate	Total variance contribution rate
1	4.01	57.32%	57.32%
2	1.38	19.68%	77.00%
3	1.02	14.46%	91.46%
4	0.21	2.96%	94.42%
5	0.18	2.56%	96.98%
6	0.16	2.24%	99.23%
7	0.05	0.77%	100%

where D_i^- is the distance of the ith sample to the negative ideal solution; D_i^+ is the distance of the ith sample to the positive ideal solution; r_{ij}^* is the weighted standardized value of the jth index in the ith sample; c_{ij}^- is the value of the jth index in the set of negative ideal solutions; c_{ij}^+ is the value of the jth index in the set of positive ideal solutions.

The water inrush index combined with Eqs. (17) and (18) is calculated:

$$\text{WIRI}_i = D_i^- / (D_i^- + D_i^+) \tag{19}$$

where WIRI_i is the water inrush index of ith sample, the larger the value, the higher the probability of water inrush.

Results and analysis

Weight calculation of PCA

The correlation coefficients of the evaluation index were calculated by Eq. (2) to construct the correlation coefficient matrix.

$$G = \begin{pmatrix} 1 & 0.03 & -0.24 & 0.36 & -0.26 & -0.19 & 0.17 \\ 0.03 & 1 & 0.77 & 0.70 & -0.26 & 0.78 & 0.83 \\ -0.24 & 0.77 & 1 & 0.49 & -0.26 & 0.82 & 0.77 \\ 0.36 & 0.70 & 0.49 & 1 & 0 & 0.54 & 0.84 \\ -0.26 & -0.26 & -0.26 & 0 & 1 & 0.19 & -0.22 \\ -0.19 & 0.78 & 0.82 & 0.54 & -0.19 & 1 & 0.81 \\ 0.17 & 0.83 & 0.77 & 0.84 & -0.22 & 0.81 & 1 \end{pmatrix} \tag{20}$$

Combined with the correlation coefficient matrix, the corresponding eigenvalues were calculated. Moreover, the corresponding contribution rates of each component were obtained (Table 1).

Table 1 shows that 7 components were extracted. The corresponding eigenvalues are 4.01, 1.38, 1.02, 0.21, 0.18, 0.16 and 0.05, respectively. Taking the feature greater than 1 as the criterion for extracting the principal components, the first three components were regarded as the principal components. Combined with the eigenvalues of the principal components, the relationship

Table 2 Standardized value of each evaluation index

Samples	Fault Fractal dimension	Coal seam dip angle	Mining depth	Dip length of panel	Aquifuge thickness	Water pressure	Water abundance
101	0.47	0.30	0.70	1	0.38	0.41	0.71
103	0.77	0.50	0.17	1	0	0.35	0.42
201	0.56	0.90	1	0.50	0.90	1	0.80
202	0.89	0.50	0.38	1	0.81	0.45	0.64
203	1	0.50	0.14	1	0.85	0.31	0.53
204	0.92	0.30	0.09	0.50	0.62	0.29	0.40
301	0.55	0.90	0.76	1	0.96	0.87	0.78
302	0.75	0.30	0.28	0.50	0.90	0.36	0.62
303	0.76	0.30	0.07	0.50	0.97	0.12	0.20
401	0.65	0.00	0.01	0.00	0.65	0.30	0.04
1002	0.75	0.30	0.05	0.50	0.93	0.28	0.29
1003	0.52	0.30	0.53	0.00	0.94	0	0.09
J1	0.59	1	0.93	1	0.91	0.98	1
J2	0.59	1	0.84	1	0.97	0.67	0.82
J3	0.59	0.50	0.69	1	1	0.83	0.87
J4	0.68	0.30	0.63	0.50	1	0.49	0.33
J5	0.98	0.30	0.18	0.50	0.90	0.28	0.31
J6	0.90	0.30	0	0.50	0.77	0.17	0.31
J7	0.88	0.30	0.25	0.50	0.91	0.32	0.27
J8	0.72	0	0.06	0	0.93	0.20	0.16
J9	0.08	0	0.22	0	0.33	0.40	0
J10	0	0.30	0.07	0	0.66	0.27	0.04

between the evaluation index and the principal components was constructed.

$$\begin{cases} cY_1 = 0.06X_1 + 0.92X_2 + 0.87X_3 - 0.79X_4 - 0.29X_5 + 0.89X_6 + 0.96X_7 \\ Y_2 = 0.97X_1 - 0.01X_2 - 0.32X_3 + 0.34X_4 - 0.36X_5 - 0.29X_6 + 0.12X_7 \\ Y_3 = 0.09X_1 - 0.02X_2 - 0.17X_3 + 0.44X_4 + 0.88X_5 - 0.05X_6 + 0.12X_7 \end{cases} \quad (21)$$

The weight of each evaluation index was determined by Eq. (4) as 0.13, 0.17, 0.11, 0.23, 0.01, 0.13 and 0.21.

Weight calculation of CRITIC

Combined with the correlation between the evaluation index and water inrush, the standardized value of each evaluation index was calculated by Eqs. (6) and (7) (Table 2).

The information amounts and weights were determined by Eqs. (9) and (10), respectively, i.e., $R = (5.60, 2.63, 3.13, 3.07, 4.81, 3.06, 2.36)^T$, $t = (1.43, 0.78, 1.03, 1.19, 1.23, 0.84, 0.71)^T$ and $\beta = (0.20, 0.11, 0.14, 0.16, 0.17, 0.12, 0.10)^T$. The combined weights of the water inrush indicators $w_j = (0.17, 0.15, 0.14, 0.21, 0.05, 0.14, 0.15)$ were defined by Eq. (14).

Construction of water inrush risk assessment model

The negative ideal solution and positive ideal solution of each evaluation index were determined as $C^- = (0, 0, 0, 0, 0.05, 0, 0)$ and $C^+ = (0.17, 0.15, 0.14, 0.21, 0, 0.14, 0.15)$, combined with the standardized value of the evaluation index and its weights. In addition, the ideal solution distance and WIRI corresponding to the sample data (Fig. 5) were obtained by Eq. (19).

Figure 5a shows that the negative ideal solution distances of 22 samples rangeed from 0.07 to 0.37. Among them, the negative ideal solution distances of J1, J2 and 301 were higher, i.e., 0.37, 0.34 and 0.32, reflecting a farther distance from low risk; however, the negative ideal solution distances of J9, J10 and 401 were lower, i.e., 0.07, 0.06 and 0.12, respectively, indicating a closer distance from less risk. Figure 5b shows that the positive ideal solution distances of samples ranged from 0.08 to 0.36. Moreover, the positive ideal solution distances of J9 and J10 were higher, with the values being both 0.36. It reveals a lower water inrush probability. However, the positive ideal solution distances of J1, J2 and 301 were smaller. their values were 0.08, 0.10, and 0.11, respectively, suggesting that a higher risk of water inrush. Figure 5c shows that the WIRI of the samples ranged from 0.15 to 0.82. Further, the WIRI values of J9 and J10 were lower i.e., 0.17 and 0.15, indicating a lower risk of water inrush. The WIRI of J1, J2 and 301 were higher, with the values being 0.82, 0.77 and 0.76 respectively, demonstrating a higher risk of water inrush.
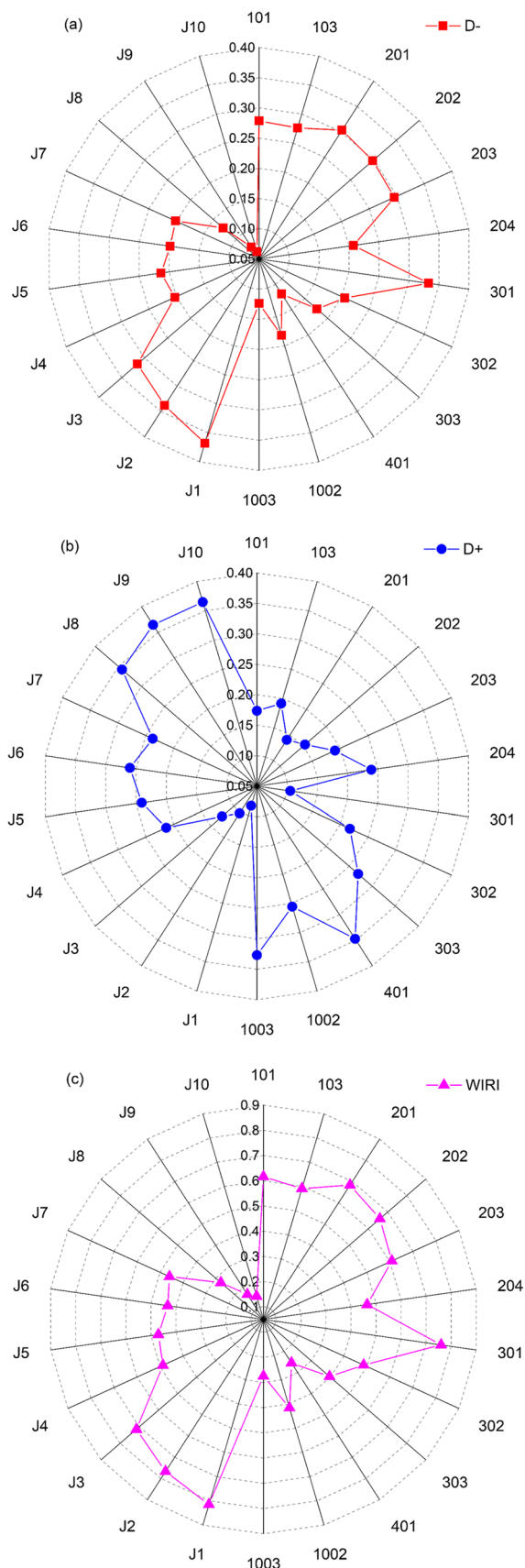

Fig. 5 Sample parameters of TOPSIS water inrush evaluation model

Division of water inrush risk areas

Combined with the WIRI of the samples, the water inrush risk zoning in the study area were determined with GIS (Fig. 6). Moreover, the thresholds of WIRI were treated with the jenks natural breaks classification method built-in GIS (Amirruddin et al. 2020). According to the difference of the intra-class and the inter-class, the interruption value of the data was determined, namely, 0.26, 0.38, 0.52 and 0.66. Therefore, the study area was classified to five areas, i.e., the safe areas, the relatively safe areas, the transitional areas, the relatively dangerous areas and the dangerous areas.

Figure 6 shows that the risk of water inrush in the study area was classified into 5 areas, namely, the safe areas $(0.15 \leq \text{WIRI} < 0.26)$, the relatively safe areas $(0.26 \leq \text{WIRI} < 0.38)$, the transitional areas $(0.38 \leq \text{WIRI} < 0.52)$, the relatively dangerous areas $(0.52 \leq \text{WIRI} < 0.66)$ and the dangerous areas $(0.66 \leq \text{WIRI} < 0.82)$. The risk of water inrush gradually decreased from northwest to southeast of the study area. Combined with the single-factor thematic map and the corresponding index weight, it can be found that the dip length of panel, water abundance, and mining depth play a greater role in the classification of water inrush risk. This leads to a high probability of water inrush in the northwest of the study area with a high risk of water inrush. In addition, there were 5 water inrush points in the study area, i.e., TS01, TS02, TS03, TS04 and TS05. These water inrush points were distributed in the

dangerous areas and the relatively dangerous areas. Judging by the principle of maximum probability, the accuracy of the WIRI evaluation model is over 90%, indicating a good fitting effect of the actual water inrush situation.

Discussions

Weight calculation comparison

The reason for the higher evaluation accuracy of the WIRI evaluation model is that it uses a variety of more scientific decision-making methods to divide the weight of evaluation indicators. Moreover, the CRITIC was used to define weights according to the conflicts and differences of sample data. Compared with the traditional entropy weight method, its weight mainly was determined by the entropy (Eq. (22)). By comparing two different weight calculation methods (Eqs. (9) and (10)), the CRITIC can combine more information of sample data to calculate weight. It improves the calculation accuracy of weight.

$$s_j = -\frac{1}{\ln m} \sum_{i=1}^{m} P_{ij} \ln P_{ij} \qquad (22)$$

where s_j is the entropy; m is the number of evaluation object; P_{ij} is the standard value of each evaluation factors. At the same

Fig. 6 Risk zoning map of floor water inrush in study area
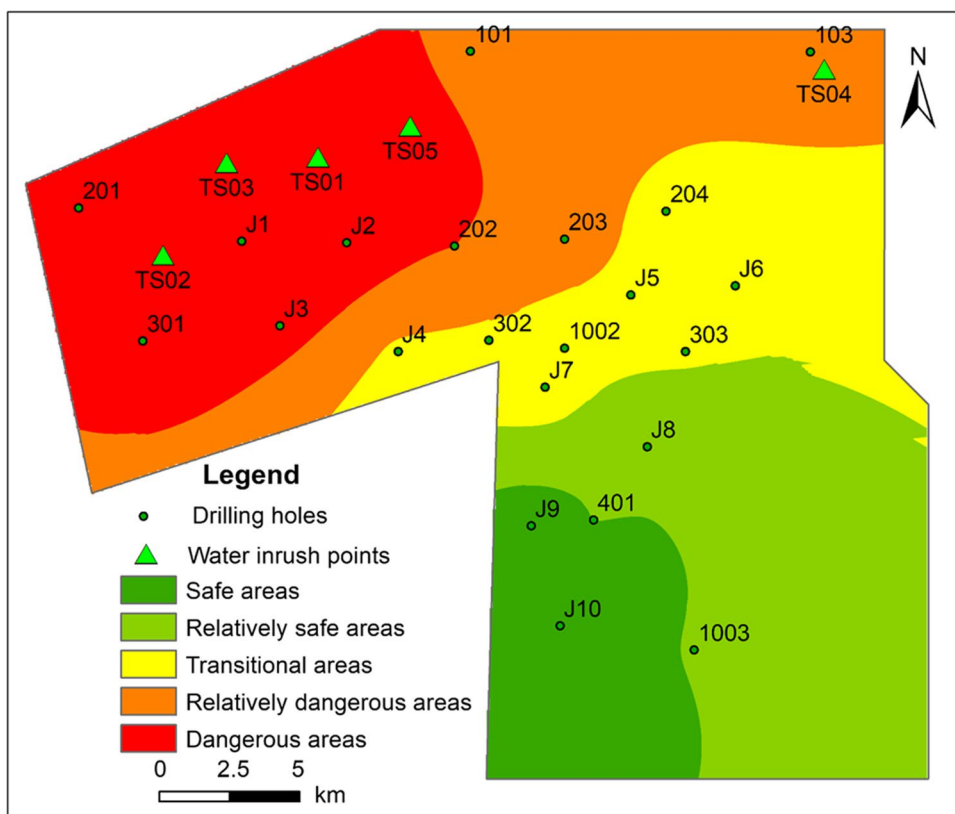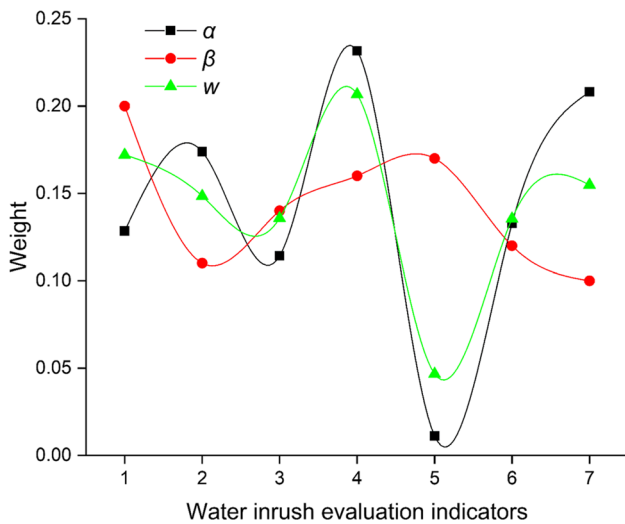
Fig. 7 Weight distribution of evaluation indicators

time, the KIC was used to superimpose the weights, ensuring the balance of comprehensive weights in various decision-making methods (Fig. 7). It improves the scientificity of weight division.

Figure 7 shows that the comprehensive weight of each evaluation index was between the weights determined by the two methods. In the PCA and the CRITIC, the weight values corresponding to the seven evaluation indicators were the same. The maximum and minimum weight values of the PCA were 0.23

and 0.01 respectively, corresponding to evaluation indicators 4 and 5; the maximum and minimum weight values of the CRITIC were 0.20 and 0.10 respectively, corresponding to evaluation indicators 1 and 7; the maximum and minimum comprehensive weights were 0.21 and 0.05 respectively, corresponding to evaluation indicators 4 and 5. It can be seen that the comprehensive weight retains the distribution characteristics of the maximum and minimum values of the evaluation indicators of the PCA weight, as well as the weight ranking characteristics of CRITIC. It can better reflect the weight of the two evaluation methods. At the same time, in the process of building the evaluation model, the multiple factors were selected as evaluation indicators to establish the evaluation index system. Compared with the traditional water inrush coefficient method, more factors were considered, which can better reflect the actual water inrush situation.

Comparative verification

To verify the accuracy of the WIRI evaluation model, the comparison with the water inrush coefficient method was carried out. Combined with the principle of the water inrush coefficient method (Wu et al. 2021b), the water inrush coefficient of the structural area is 0.06 Mpa/m; the water inrush coefficient of the complete block area is 0.10 Mpa/m. Due to the relatively developed structure in the study area, the 0.06 Mpa/m was selected as the threshold for the division of water inrush risk areas (Fig. 8).

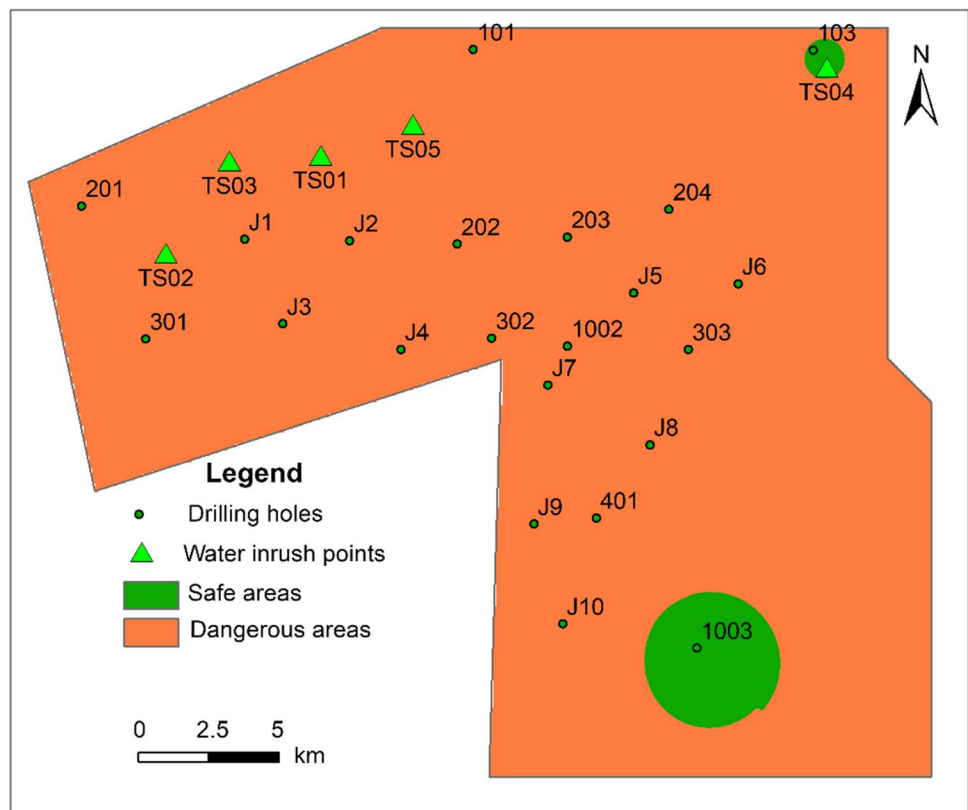**Fig. 8** Risk zoning map of water inrush coefficient method

Figure 8 shows that the study area was divided into two areas, namely, the safe areas and the dangerous areas, according to the water inrush threshold of 0.06 Mpa/m. It can be seen that the dangerous areas occupied most of the study area, while the safe areas occupied a smaller part of the study area. In addition, only one water inrush point was located in the safe area, i.e., 103, implying a phenomenon inconsistent with the actual water inrush situation. If the water inrush risk of study area is distinguished by the water inrush coefficient method, there will be a large error in the actual situation of water inrush. In comparison, the prediction accuracy of the WIRI evaluation model is higher. it fits the actual water inrush situation better, with a higher accuracy. This model can provide a better guarantee for safe coal mining on confined water.

Conclusions

The WIRI evaluation model based on PCA and CRITIC was proposed. The main findings are as follows:

The geological and hydrogeological conditions of the study area were analyzed. 7 factors were selected as water inrush evaluation indicators to construct a water inrush evaluation system i.e., the fault fractal dimension, the coal seam dip angle, the mining depth, the dip length of panel, the aquifuge thickness, the water pressure and the water abundance.

The PCA extracted three principal components with a contribution of 91.46% to determine the weight of the water inrush evaluation index. The information contained in the evaluation index was relatively high. The CRITIC calculated the conflict, information and other parameters of the water inrush evaluation index to determine its weight. It makes the weight determination more objective. The combined weight was constructed by the KIC, resulting in a more scientific weight determination. By constructing a WIRI evaluation model, the study area was classified into the safe areas, the relatively safe areas, the transitional areas, the relatively dangerous areas and the dangerous areas. The fitting effect is good with the actual water inrush, with a prediction accuracy being over 90%. Compared with the water inrush coefficient method, its prediction accuracy is higher. The model provides guidance for the prevention of the floor water hazards and theoretical support for the safe coal mining above confined water.

Declarations

References

Amirruddin AD, Muharam FM, Ismail MH, Ismail MF, Tan NP, Karam DS (2020) Hyperspectral remote sensing for assessment of chlorophyll sufficiency levels in mature oil palm (Elaeis guineensis) based on frond numbers: analysis of decision tree and random forest. Comput Electron Agric 169:105221. https://doi.org/10.1016/j.compag.2020.105221

Baykasoğlu A, Gölcük İ (2017) Development of an interval type-2 fuzzy sets based hierarchical MADM model by combining DEMATEL and TOPSIS. Expert Syst Appl 70:37–51. https://doi.org/10.1016/j.eswa.2016.11.001

Casagrande MFS, Moreira CA, Targa DA (2020) Study of generation and underground flow of acid mine drainage in waste rock pile in an Uranium Mine using electrical resistivity tomography. Pure Appl Geophys 177:703–721. https://doi.org/10.1007/s00024-019-02351-9

Chen L, Feng X, Xu D, Zeng W, Zheng Z (2018) Prediction of water inrush areas under an unconsolidated, confined aquifer: the application of multi-information superposition Based on GIS and AHP in the Qidong coal mine, China. Mine Water Environ 37(4):786–795. https://doi.org/10.1007/s10230-018-0541-1

Diakoulaki D, Mavrotas G, Papayannakis L (1995) Determining objective weights in multiple criteria problems: the critic method. Comput Oper Res 22:763–770. https://doi.org/10.1016/0305-0548(94)00059-H

Donnelly LJ (2006) A review of coal mining induced fault reactivation in Great Britain. Q J Eng Geol Hydrogeol 39(1):5–50. https://doi.org/10.1144/1470-9236/05-015

Duan HF, Zhao LJ (2021) New evaluation and prediction method to determine the risk of water inrush from mining coal seam floor. Environ Earth Sci 80:30. https://doi.org/10.1007/s12665-020-09339-y

Gao CY, Wang DL, Liu KR, Deng GW, Li JF, Jie BL (2022) A multifactor quantitative assessment model for safe mining after roof drainage in the Liangshuijing coal mine. ACS Omega 7:26437–26454. https://doi.org/10.1021/acsomega.2c02270

He JH, Li WP, Qiao W, Yang Z, Wang QQ (2021) Risk assessment of water inrushes from bed separations in Cretaceous strata corresponding to different excavation lengths during mining in the Ordos Basin. Geomatics Nat Hazards Risk 12(1):2300–2327. https://doi.org/10.1080/19475705.2021.1950220

Hu YB, Li WP, Wang QQ, Liu SL, Wang ZK (2019) Evaluation of water inrush risk from coal seam floors with an AHP–EWM algorithm and GIS. Environ Earth Sci 78:290. https://doi.org/10.1007/s12665-019-8301-5

Hu YB, Li WP, Liu SL, Wang QQ (2021) Prediction of floor failure depth in deep coal mines by regression analysis of the multi-factor influence index. Mine Water Environ 40:497–509. https://doi.org/10.1007/s10230-021-00769-z

Ju QD, Hu YB (2021) Source identification of mine water inrush based on principal component analysis and grey situation decision. Environ Earth Sci 80:157. https://doi.org/10.1007/s12665-021-09459-z

Li B, Wu Q, Duan XQ, Chen MY (2018) Risk analysis model of water inrush through the seam floor based on set pair analysis. Mine Water Environ 37:281–287. https://doi.org/10.1007/s10230-017-0498-5

Li B, Wu Q, Liu ZJ (2020) Identification of Mine Water Inrush Source Based on PCA-FDA: Xiandewang Coal Mine Case. Geofluids 2020:2584094. https://doi.org/10.1155/2020/2584094

Li SC, Liu C, Zhou ZQ, Li LP, Shi SS (2021) Multi-sources information fusion analysis of water inrush disaster in tunnels based on improved theory of evidence. Tunn Undergr Space Technol 113:103948. https://doi.org/10.1016/j.tust.2021.103948

Liu WT, Li Q, Zhao JY, Fu B (2018a) Assessment of water inrush risk using the principal component logistic regression model in the Pandao coal mine. China Arab J Geosci 11(16):463. https://doi.org/10.1007/s12517-018-3815-9

Liu WT, Mu DR, Xie XX, Yang L et al (2018b) Sensitivity analysis of the main factors controlling floor failure depth and a risk evaluation of floor water inrush for an inclined coal seam. Mine Water Environ 37:636–648. https://doi.org/10.1007/s10230-017-0497-6

Liu GW, Ma FS, Liu G, Zhao HJ, Guo J, Gao JY (2019) Application of multivariate statistical analysis to identify water sources in a Coastal Gold Mine, Shandong, China. Sustainability 11(12):3345. https://doi.org/10.3390/su11123345

Liu JW, Zhang DY, Yang BB, Liu S, Wang Y, Xu K (2020) Suitability of aquifer-protection mining in ecologically fragile areas in western China. Environ Earth Sci 79:356. https://doi.org/10.1007/s12665-020-09098-w

Mahato MK, Singh PK, Singh AK, Tiwari AK (2018) Assessment of hydrogeochemical processes and mine water suitability for domestic, irrigation, and industrial purposes in east Bokaro coalfield, India. Mine Water Environ 37:493–504. https://doi.org/10.1007/s10230-017-0508-7

Niu HG, Wei JC, Yin HY, Xie DL, Zhang WJ (2020) An improved model to predict the water-inrush risk from an Ordovician limestone aquifer under coal seams: a case study of the Longgu coal mine in China. Carbonates Evaporites 35:73. https://doi.org/10.1007/s13146-020-00590-9

Norouzi A, Namin HG (2019) A hybrid fuzzy TOPSIS-best worst method for risk prioritization in megaprojects. Civil Eng J 5(6):1257–1272. https://doi.org/10.28991/cej-2019-03091330

Osses A, Gallardo L, Faundez T (2013) Analysis and evolution of air quality monitoring networks using combined statistical information indexes. Tellus B: Chem Phys Meteorol 65:19822. https://doi.org/10.3402/tellusb.v65i0.19822

Pearson K (1901) On lines and planes of closest fit to systems of points in space. Philos Mag 2(2):559–572. https://doi.org/10.1080/14786440209462785

Qiu M, Huang FJ, Wang Y, Guan T, Shi LQ, Han J (2020) Prediction model of water yield property based on GRA, FAHP and TOPSIS methods for Ordovician top aquifer in the Xinwen coalfield of China. Environ Earth Sci 79:214. https://doi.org/10.1007/s12665-020-08954-z

Qu XY, Shi LQ, Qu XW, Bilal A, Qiu M, Gao WF (2021) Multi-model fusion for assessing risk of inrush of limestone karst water through the mine floor. Energy Rep 7:1473–1487. https://doi.org/10.1016/j.egyr.2021.02.052

Salifu A, Petrusevski B, Ghebremichael K, Buamah R, Amy G (2012) Multivariate statistical analysis for fluoride occurrence in groundwater in the northern region of Ghana. J Contam Hydrol 140–141:34–44. https://doi.org/10.1016/j.jconhyd.2012.08.002

Shi LQ, Tan XP, Wang J, Ji XK, Niu C, Xu DJ (2015) Risk assessment of water inrush based on PCA_Fuzzy_PSO_SVC. J Chin Coal Soc 40(1):167–171

Shi LQ, Qiu M, Teng C, Wang Y, Liu TH, Qu XY (2020) Risk assessment of water inrush to coal seams from underlyingaquifer by an innovative combination of the TFN-AHP and TOPSIS techniques. Arab J Geosci 13:600. https://doi.org/10.1007/s12517-020-05588-0

Sun Q, Meng GH, Sun K, Zhang JX (2020) Physical simulation experiment on prevention and control of water inrush disaster by backfilling mining under aquifer. Environ Earth Sci 79:429. https://doi.org/10.1007/s12665-020-09174-1

Thiesen S, Darscheid P, Ehret U (2019) Identifying rainfall-runoff events in discharge time series: a data-driven method based on information theory. Hydrol Earth Syst Sci 23:1015–1034. https://doi.org/10.5194/hess-23-1015-2019

Wang JA, Park HD (2003) Coal mining above a confined aquifer. Int J Rock Mech Min Sci 40(4):537–551. https://doi.org/10.1016/S1365-1609(03)00029-7

Wang F, Chen T, Ma B, Chen DH (2021) Formation mechanism of stress arch during longwall mining based on key strata theory. Energy Explor Exploit 40(2):816–833. https://doi.org/10.1177/01445987211042701

Wu Q, Guo XM, Shen JJ, Xu S, Liu SQ, Zeng YF (2017) Risk assessment of water inrush from aquifers underlying the Gushuyuan coal mine, China. Mine Water Environ 36:96–103. https://doi.org/10.1007/s10230-016-0410-8

Wu TH, Gao YT, Zhou Y, Sun H (2021a) A novel comprehensive quantitative method for various geological disaster evaluations in underground engineering: multidimensional finite interval cloud model (MFICM). Environ Earth Sci 80:696. https://doi.org/10.1007/s12665-021-10012-1

Wu WL, Liu XL, Guo JQ, Sun FY, Huang X, Zhu ZG (2021b) Upper limit analysis of stability of the water-resistant rock mass of a karst tunnel face considering the seepage force. Bull Eng Geol Env 80:5813–5830. https://doi.org/10.1007/s10064-021-02283-6

Xu ZG, Xian MT, Li XF, Zhou W, Wang JM, Wang YP, Chai JR (2021) Risk assessment of water inrush in karst shallow tunnel with stable surface water supply: Case study. Geomech Eng 25(6):495–508. https://doi.org/10.12989/gae.2021.25.6.495

Yang BB, Yuan JH, Duan LH (2018) Development of a system to assess vulnerability of flooding from water in karst aquifers induced by mining. Environ Earth Sci 77:91. https://doi.org/10.1007/s12665-018-7275-z

Yu S, Ding HH, Zeng YF (2022) Evaluating water-yield property of karst aquifer based on the AHP and CV. Sci Rep 12:3308. https://doi.org/10.1038/s41598-022-07244-x

Zhang J, Wu Q, Mu W, Du Y, Tu K (2019) Integrating the hierarchy variable- weight model with collaboration-competition theory for assessing coal-floor water-inrush risk. Environ Earth Sci 78:1–13. https://doi.org/10.1007/s12665-019-8217-0

Zhang QY, Xu PP, Qian H (2020) Groundwater quality assessment using improved water quality index (WQI) and human health risk (HHR) evaluation in a semi-arid region of Northwest China. Exposure Health 12:487–500. https://doi.org/10.1007/s12403-020-00345-w

Zhang QY, Qian H, Xu PP, Hou K, Yang FX (2021) Groundwater quality assessment using a new integrated-weight water quality index (IWQI) and driver analysis in the Jiaokou Irrigation District, China. Ecotoxicol Environ Safety 212:111992. https://doi.org/10.1016/j.ecoenv.2021.111992

Zhang Y, Tang SF, Shi K (2022) Risk assessment of coal mine water inrush based on PCA-DBN. Sci Rep 12:1370. https://doi.org/10.1038/s41598-022-05473-8

Zhou BH, Xue YG, Li ZQ, Gao HD, Su MX, Qiu DH, Kong FM (2022) A two-step interval risk assessment method for water inrush during seaside tunnel excavation. Geomech Eng 28(6):573–584. https://doi.org/10.12989/gae.2022.28.6.573